Diagenesis in tephra-rich sediments from the Lesser Antilles Volcanic Arc: Pore fluid constraints

Murray, Natalie A.; McManus, James; Palmer, Martin R.; Haley, Brian; Manners, Hayley

Published in:
Geochimica et Cosmochimica Acta

DOI:
10.1016/j.gca.2018.02.039

Publication date:
2018

Document version:
Other version

Figure 1. Map of the Lesser Antilles Volcanic Arc, showing arc migration over time, active volcanoes, and flank collapses. Ages of migrating arc are from Macdonald et al. (2000), flank collapses are modified from Le Friant et al. (2015), and volcano locations are from the Smithsonian Institution, Global Volcanism Program. Gridded bathymetry is in meters and courtesy of the British Oceanographic Data Centre (gebco.net).

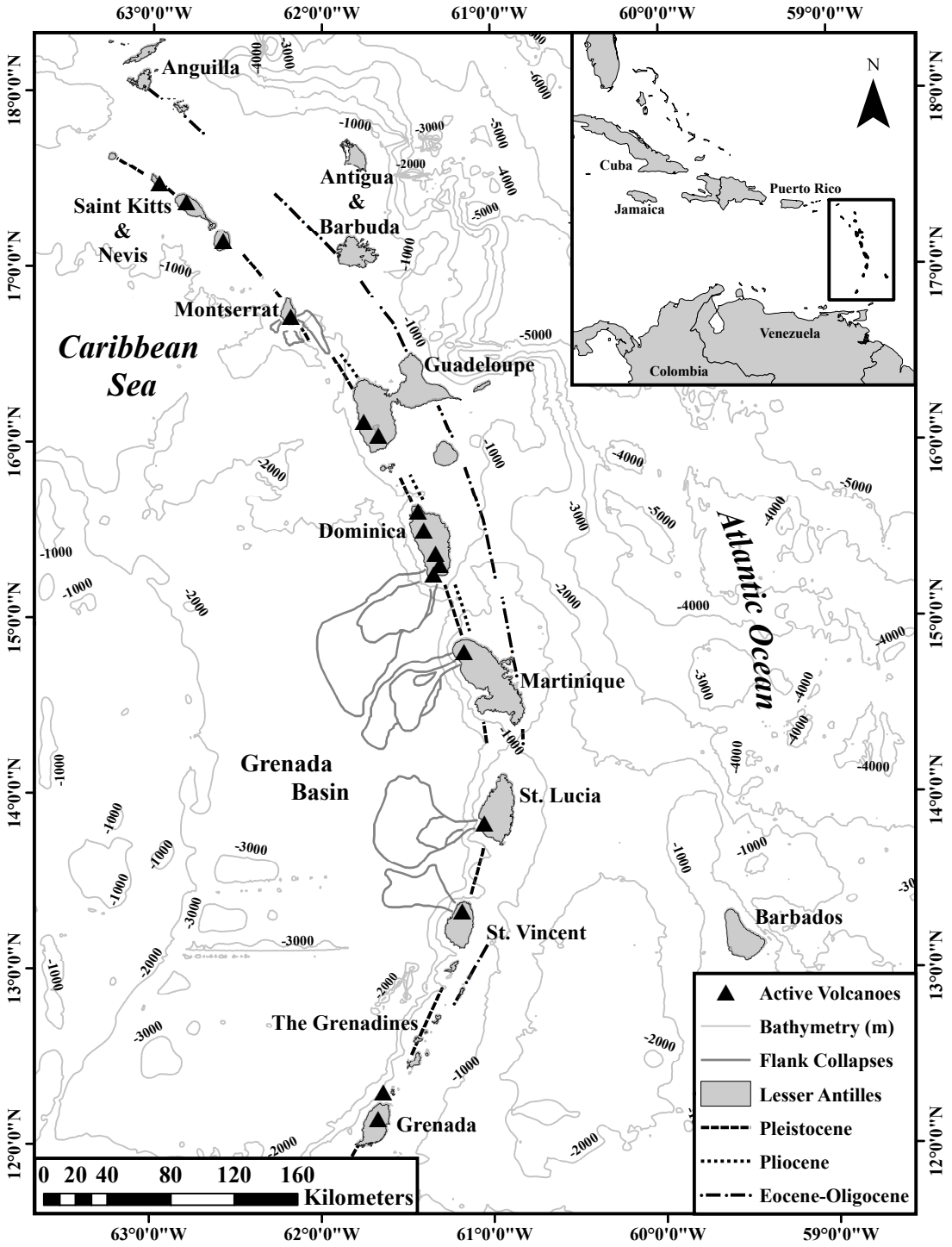

Figure 2. Close up of the study area from Expedition 340 cruise in 2012, showing the core locations of interest for this study (U1394, U1395, U1396, U1397, U1398, U1399, and U1400). Flank collapses are modified from Le Friant et al. (2015), volcano locations are from the Smithsonian Institution, Global Volcanism Program, and core coordinates from Expedition 340 Scientists (2012). Gridded bathymetry is in meters and courtesy of the British Oceanographic Data Centre (gebco.net).

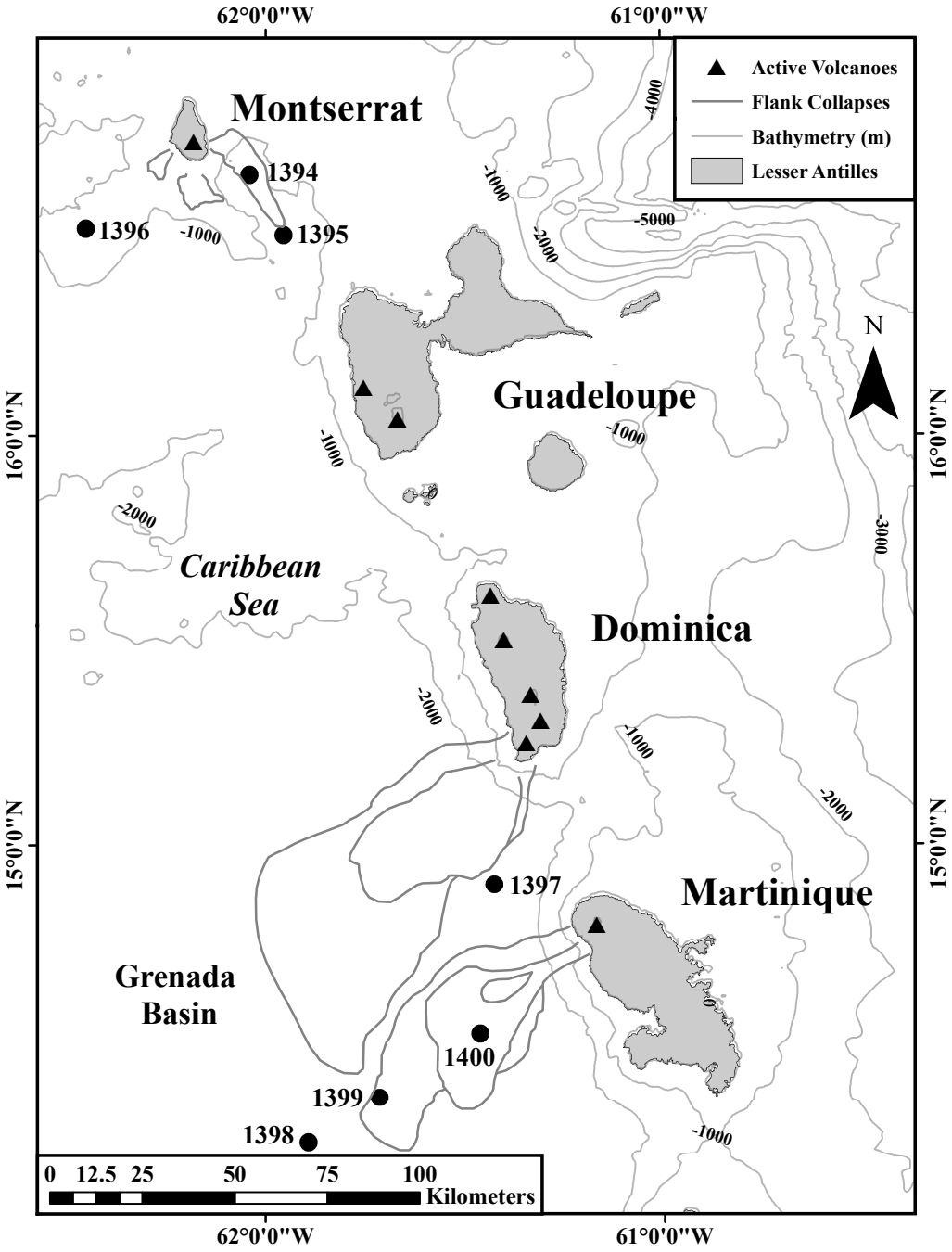

Figure 3. Dissolved solute distributions for Site U1394. (A) Alkalinity and NH_4, (B) SO_4^{2-} and Mn, (C) Ca and Mg, (D) K and Li, (E) Si, and (F) Sr. Dashed lines denote bottom water concentrations. Alkalinity, NH_4, Ca, Mg, and SO_4^{2-} data are from Le Friant et al. (2013) and minor ion data is from Murray et al. (2016).

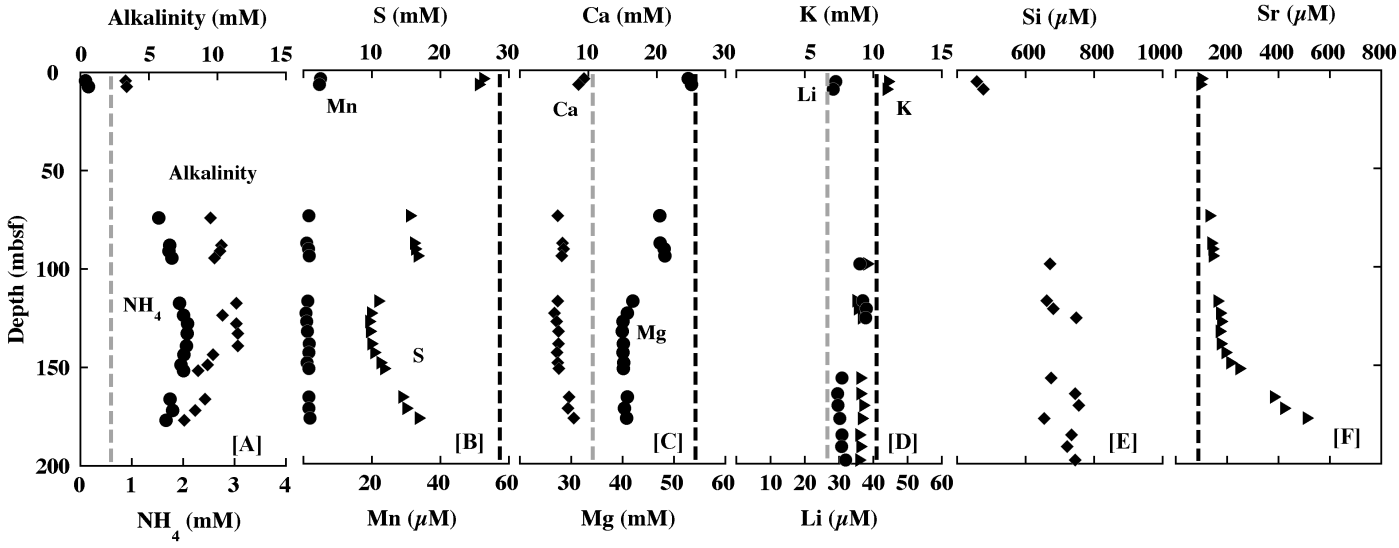

Figure 4. Dissolved solute distributions for Site U1395. (A) Alkalinity and NH_4, (B) SO_4^{2-} and Mn, (C) Ca and Mg, (D) K and Li, (E) Si, and (F) Sr. Dashed lines denote bottom water concentrations. Alkalinity, NH_4, Ca, Mg, and SO_4^{2-} data are from Le Friant et al. (2013) and minor ion data is from Murray et al. (2016).

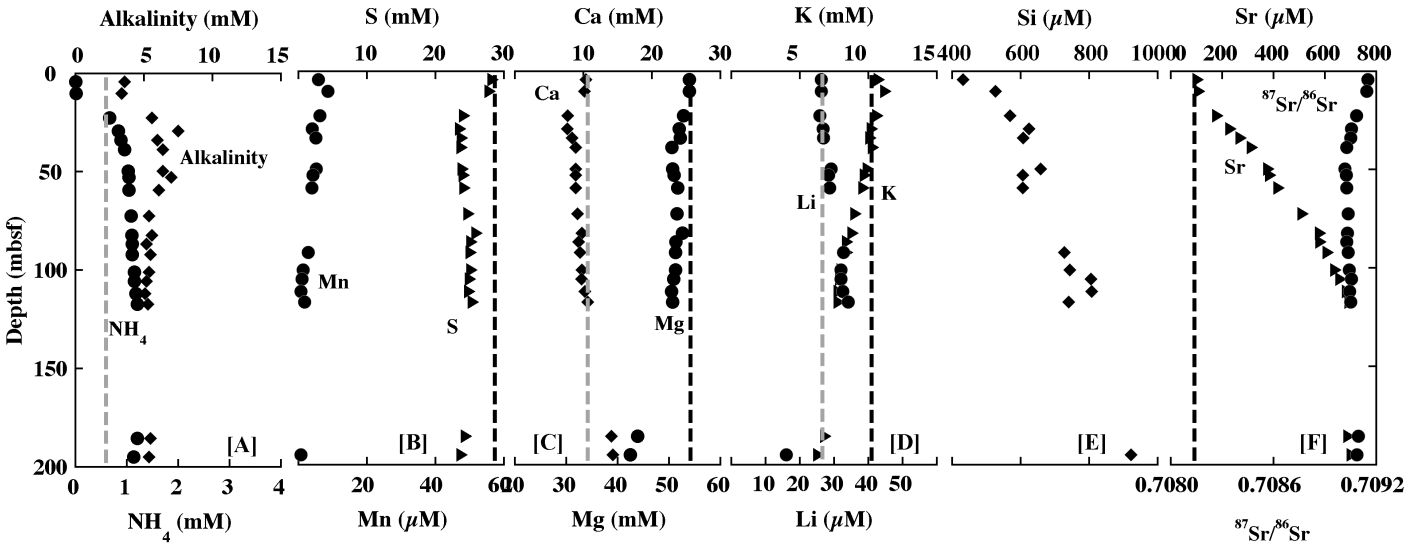

Figure 5. Dissolved solute distributions for Site U1396. (A) Alkalinity and NH_4, (B) SO_4^{2-} and Mn, (C) Ca and Mg, (D) K and Li, (E) Si, and (F) Sr. Dashed lines denote bottom water concentrations. Alkalinity, NH_4, Ca, Mg, and SO_4^{2-} data are from Le Friant et al. (2013) and minor ion data is from Murray et al. (2016).

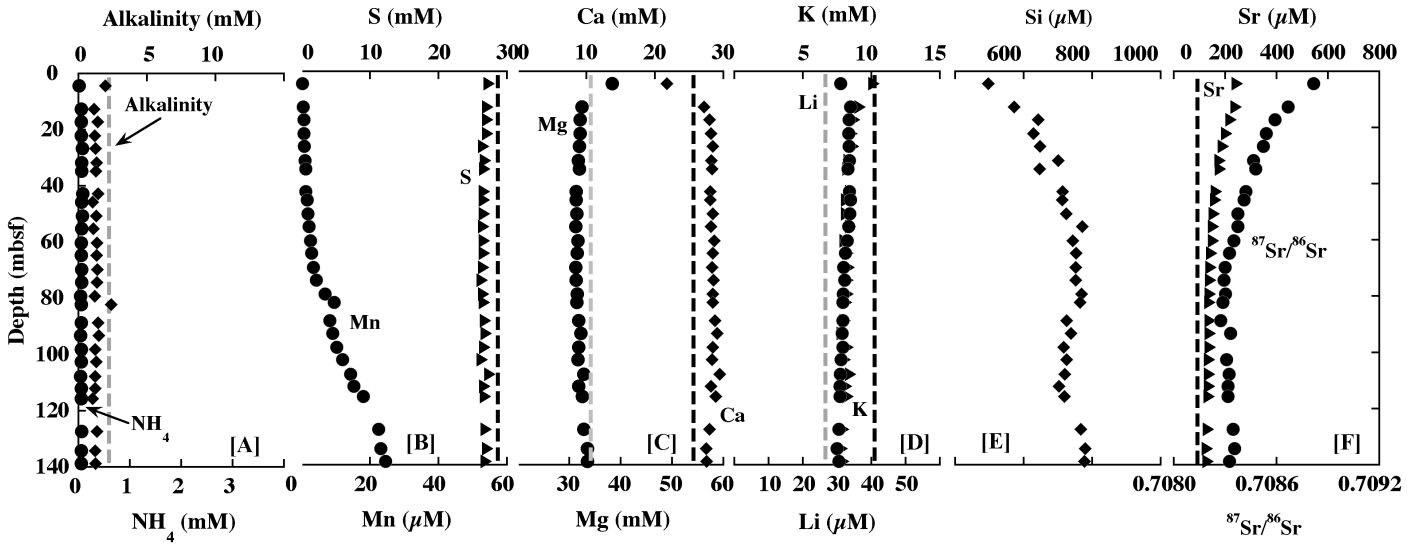

Figure 6. Dissolved solute distributions for Site U1397. (A) Alkalinity and NH_4, (B) SO_4^{2-} and Mn, (C) Ca and Mg, (D) K and Li, (E) Si, and (F) Sr and $^{87}Sr/^{86}Sr$. Dashed lines denote bottom water concentrations. Alkalinity, NH_4, Ca, Mg, and SO_4^{2-} data are from Le Friant et al. (2013) and minor ion data is from Murray et al. (2016).

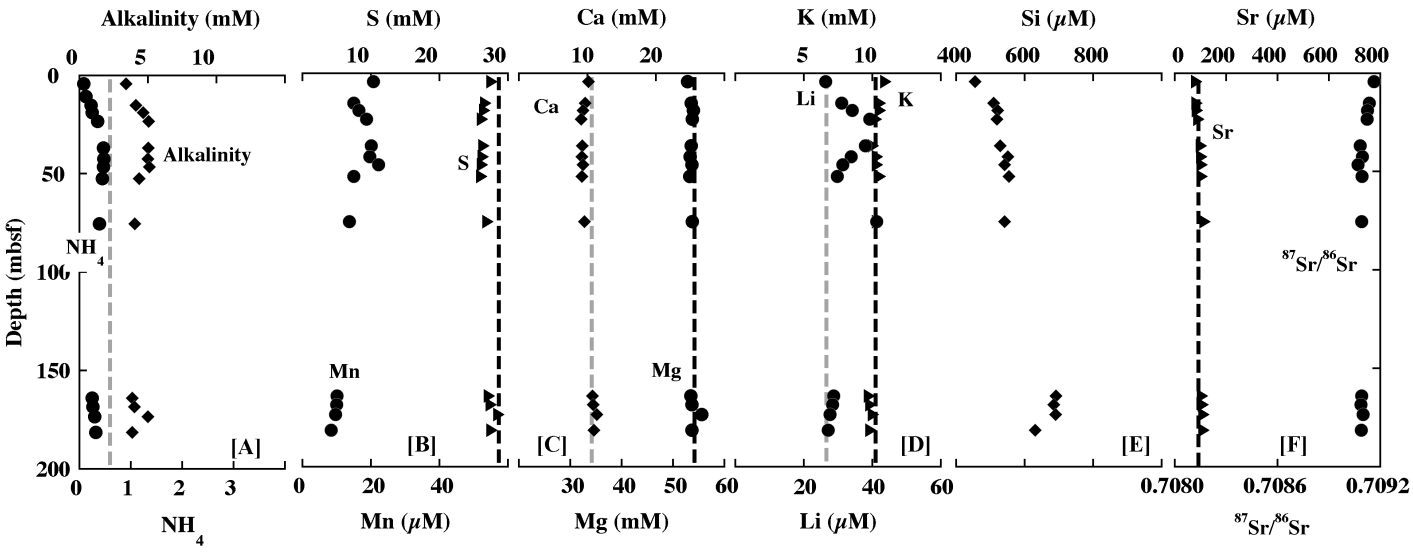

Figure 7. Dissolved solute distributions for Site U1398. (A) Alkalinity and NH_4, (B) SO_4^{2-} and Mn, (C) Ca and Mg, (D) K and Li, (E) Si, and (F) Sr and $^{87}Sr/^{86}Sr$. Dashed lines denote bottom water concentrations. Alkalinity, NH_4, Ca, Mg, and SO_4^{2-} data are from Le Friant et al. (2013) and minor ion data is from Murray et al. (2016).

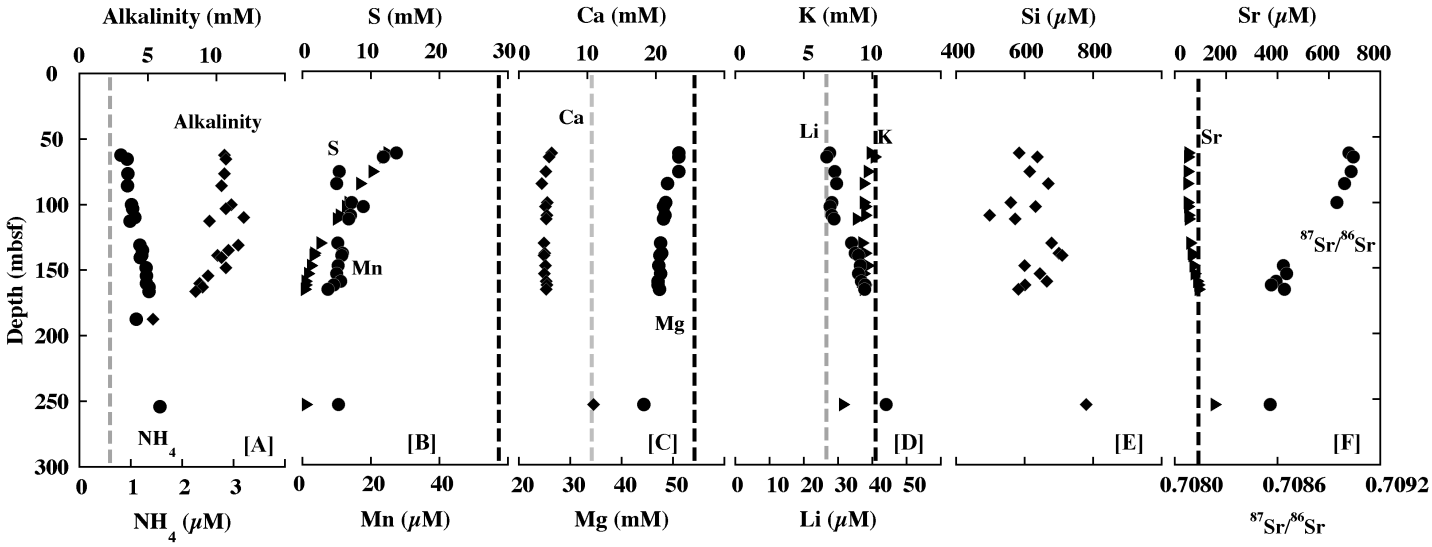

Figure 8. Dissolved solute distributions for Site U1399. (A) Alkalinity and NH_4, (B) SO_4^{2-} and Mn, (C) Ca and Mg, (D) K and Li, (E) Si, and (F) Sr and $^{87}Sr/^{86}Sr$. Dashed lines denote bottom water concentrations. Alkalinity, NH_4, Ca, Mg, and SO_4^{2-} data are from Le Friant et al. (2013) and minor ion data is from Murray et al. (2016).

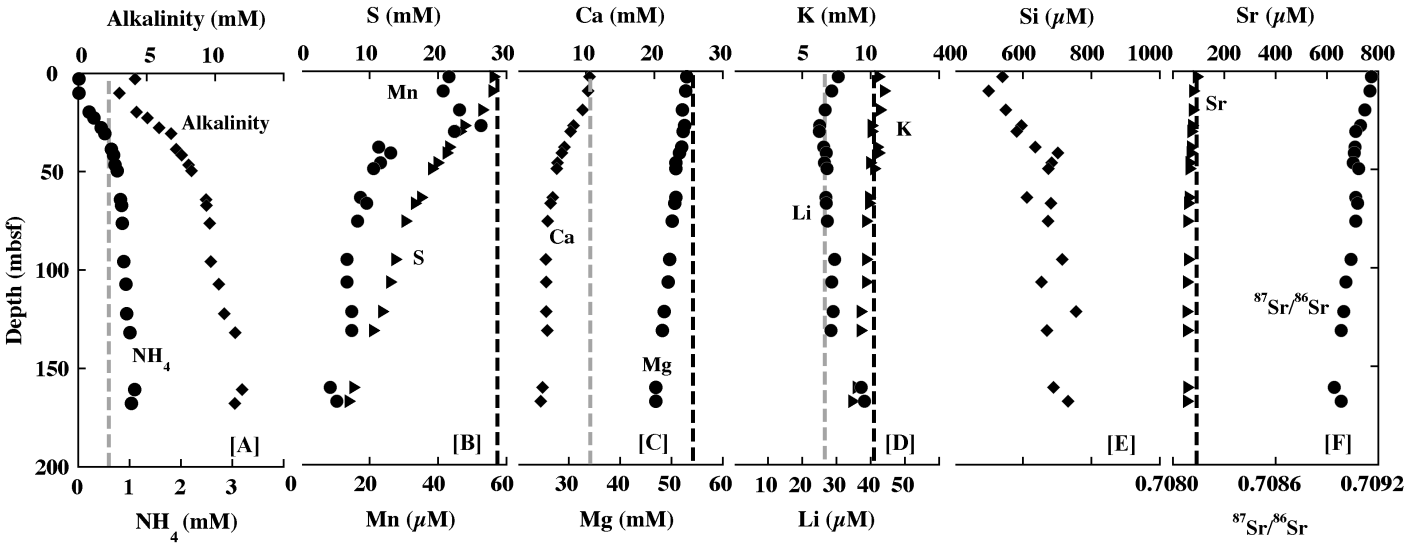

Figure 9. Dissolved solute distributions for Site U1400. (A) Alkalinity and NH_4, (B) SO_4^{2-} and Mn, (C) Ca and Mg, (D) Si and Li, and (E) Sr and $^{87}Sr/^{86}Sr$. Dashed lines denote bottom water concentrations. Alkalinity, NH_4, Ca, Mg, and SO_4^{2-} data are from Le Friant et al. (2013) and minor ion data is from Murray et al. (2016).

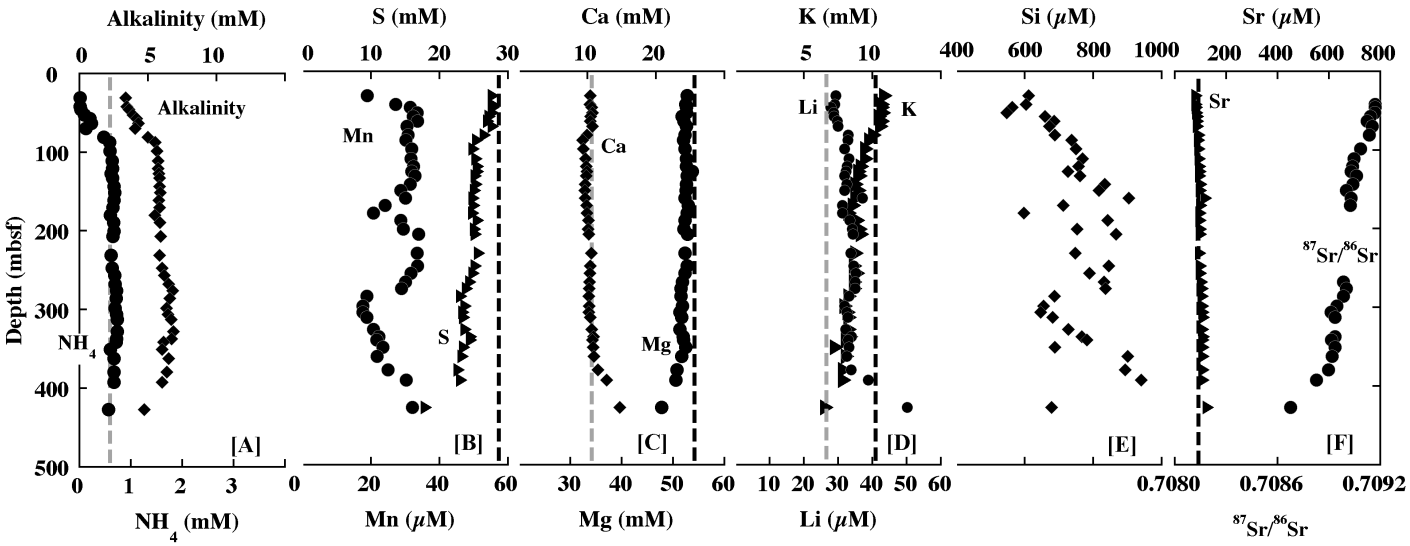

Figure 10. $^{87}Sr/^{86}Sr$ in fluids and solid phases plotted as a function of age from Site U1396. Data are from the carbonate fraction, the residual non-carbonate fraction, and the pore fluids. Age calculations are derived from (Hatfield, 2015; Coussens et al., 2016) and dashed line represents the strontium isotope value of contemporaneous seawater (Elderfield, 1982; Paytan et al., 1993).

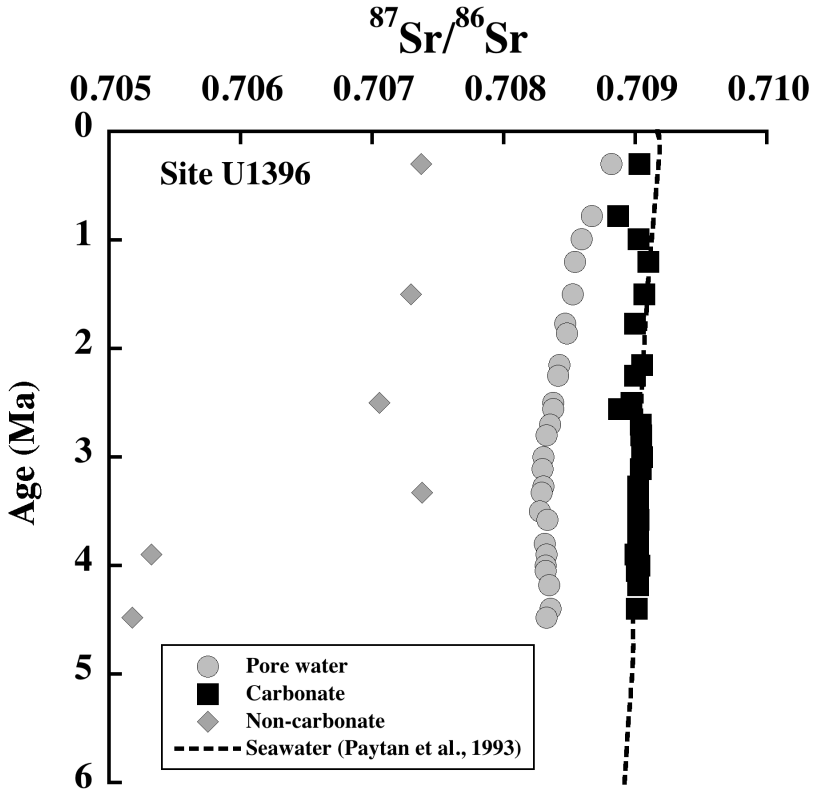

Figure 11. Dissolved Mg and Ca displaying the two dominant diagenetic reactions occurring in the Grenada Basin for the [A] northern sites U1394, U1395, and U1396 [B] southern sites U1399 and U1400. Data from sites 998, 999, 1000, and 1001 are plotted with data from this study for comparison [C, D] and are taken from Lyons et al. (2000). Data from site 671, which lies to the east within the northern Barbados accretionary complex are from Gieskes et al., 1990a.

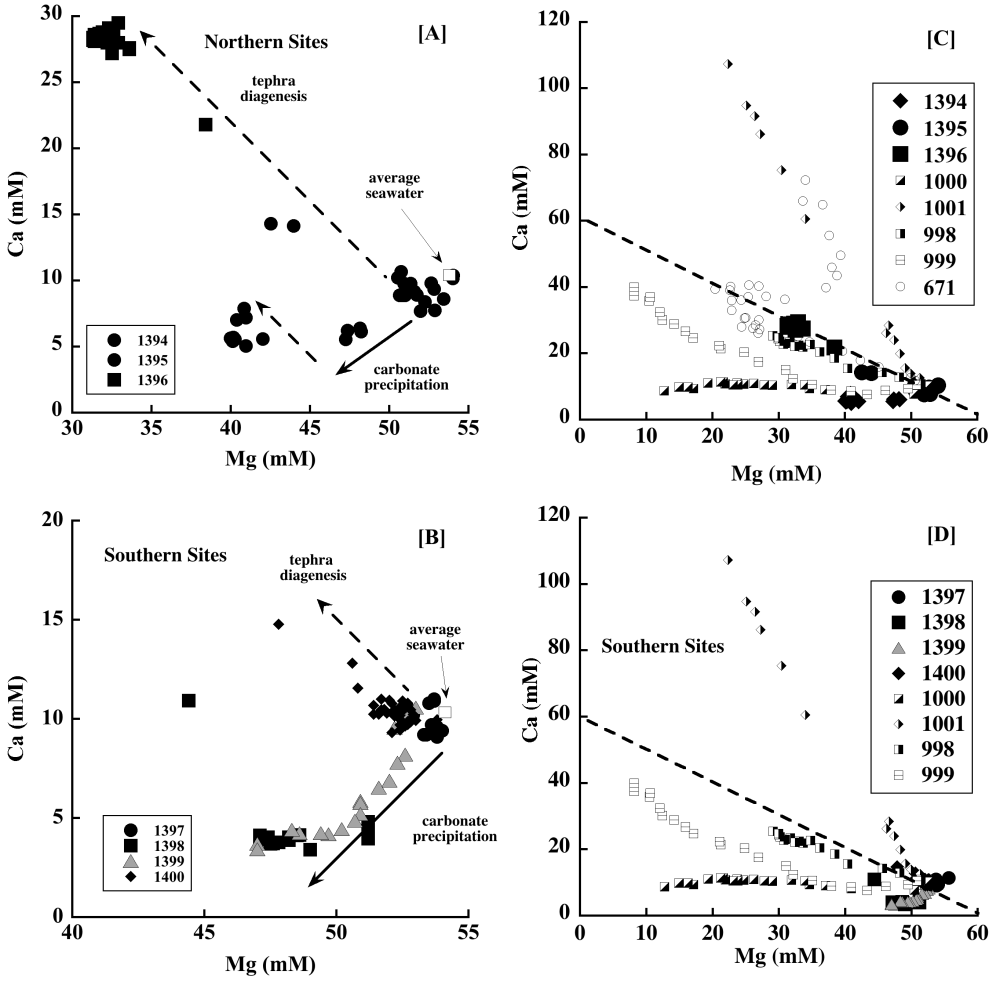

Figure 12. $^{87}Sr/^{86}Sr$ plotted as a function of 1/Sr in pore fluids. The gray box indicates Sr isotope compositions characteristic of the most recent ~4 Ma (Elderfield, 1986). Data to the right of the figure are those exhibiting removal of Sr from pore fluids, relative to the seawater value. Data to the left of the figure are those samples exhibiting Sr enrichment in the pore fluids. Note that the Sr isotope values of the pore waters at Site U1396 have the lowest $^{87}Sr/^{86}Sr$ values of any of the cores suggesting that this site is the most impacted by reaction with volcanogenic material.

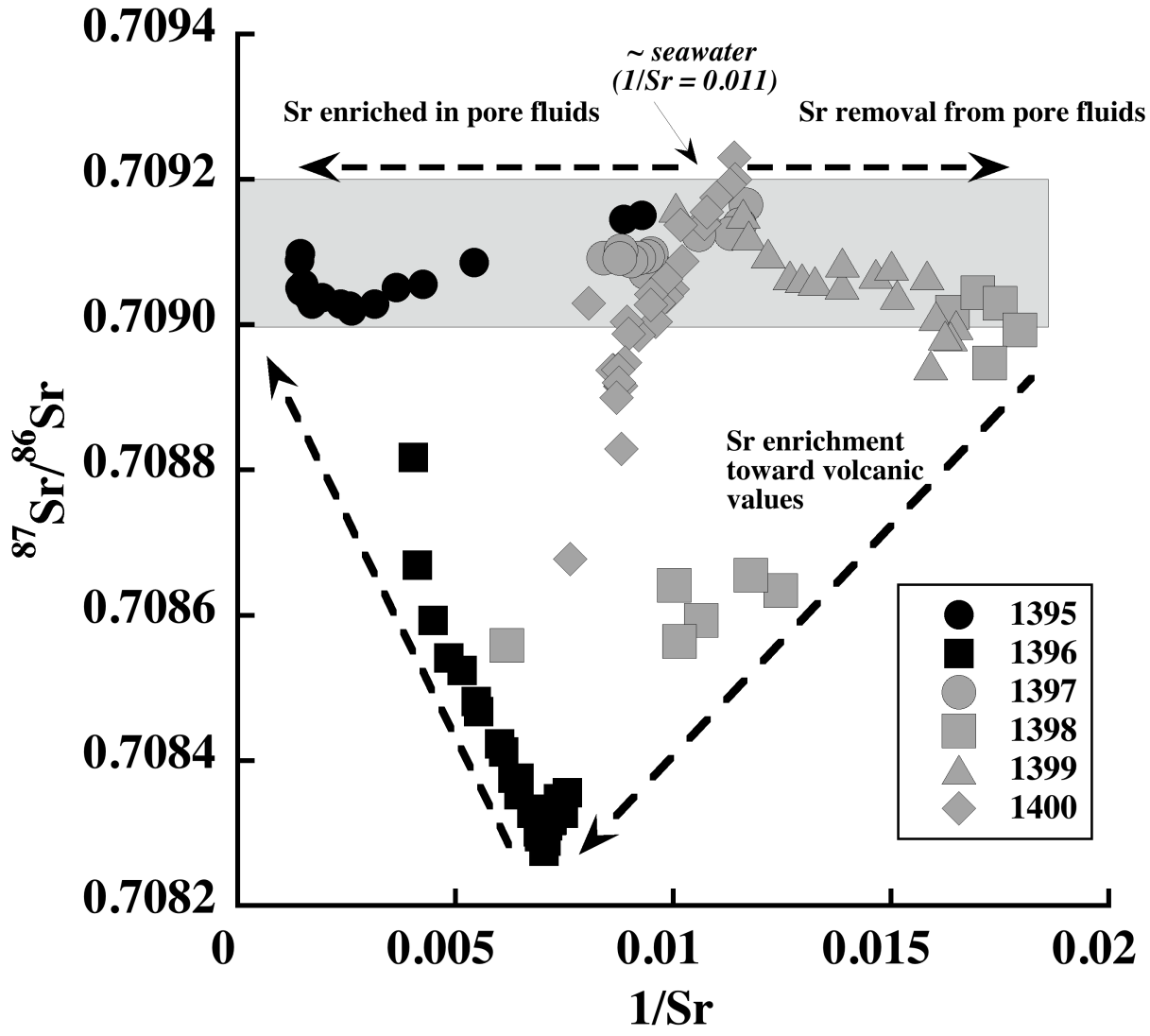

Figure 13. Calcite and aragonite saturation state calculations for sites U1394, 1398, and 1399. Note that most values are supersaturated with respect to calcite; however, the large uncertainties in these calculations, including the values for pH, likely mean that the relative saturation states are uncertain, as discussed within the text.

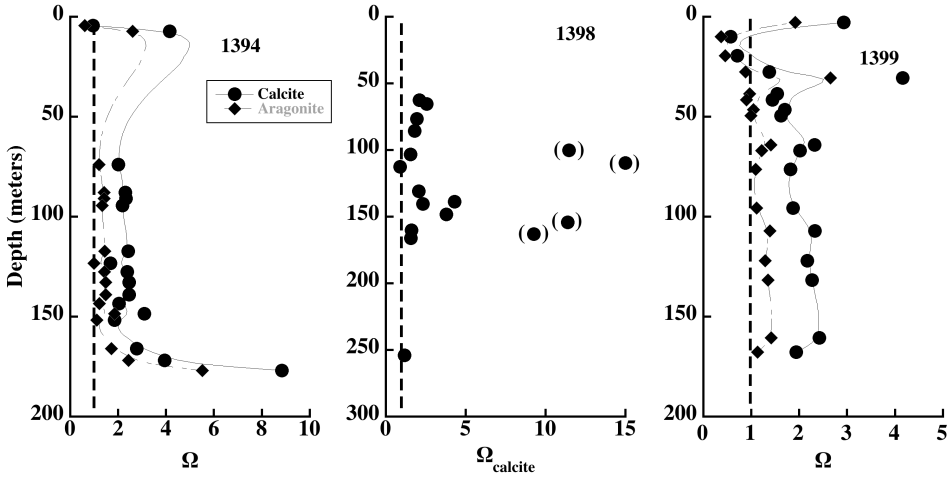

Figure 14. Dissolved minor phases that can be incorporated into the carbonate phase; (A) Mn for site U1394 (B) Mn and Sr for site U1399. Note that there is not a correlation between Sr and Ca for site U1394, which may imply that carbonate precipitation is not what is driving the correlation for site U1399.